

# The Effect of Different Concentration of Brij 35 Non-ionic Surfactant on Emulsion Polymerisation of Polyacrylamide (PAM)

Nurul Syafieqah Misdi<sup>1</sup>, Nurfarah Aini Mocktar<sup>1</sup> and  
Noor Aniza Harun<sup>1,2\*</sup>

<sup>1</sup>Faculty of Science and Marine Environment, University Malaysia Terengganu, 21030 Kuala Nerus, Terengganu, Malaysia

<sup>2</sup>Advanced Nano Materials (ANOMA) Research Group, Faculty of Science and Marine Environment, University Malaysia Terengganu, 21030 Kuala Nerus, Terengganu, Malaysia

\*Corresponding author (e-mail: nooraniza@umt.edu.my)

Polyacrylamide (PAM), a synthetic biodegradable polymer derived from acrylamide (AM) monomers, has piqued the interest of researchers in various applications because of its unique physical, chemical, and thermal properties. PAM was successfully synthesised via an emulsion polymerisation technique using different concentrations of Brij 35 as a non-ionic surfactant and ammonium persulphate (APS) as a water-soluble initiator. The effects of different concentrations of non-ionic surfactant on the formation and thermal stability of PAM were discussed. All samples were characterised by Fourier transform infrared spectroscopy (FTIR), thermogravimetric analysis (TGA) and scanning electron microscopy (SEM) analysis. The FTIR spectra exhibited prominent absorption bands such as  $\nu(\text{C-H})$ ,  $\nu(\text{C=O})$ ,  $\nu(\text{CH}_2)$  and  $\nu(\text{N-H})$  at  $2924\text{ cm}^{-1}$ ,  $1638\text{ cm}^{-1}$ ,  $1465\text{ cm}^{-1}$  and  $3326\text{ cm}^{-1}$ , respectively. TGA analysis revealed that the percentage of mass loss varied at different temperatures ranging from 30 - 600 °C. SEM analysis showed substantial aggregations of PAM particles in bulblike structures with average diameters of 5 – 100  $\mu\text{m}$ . Thus the concentration of Brij 35 had a significant effect on the formation and thermal stability of PAM.

**Keywords:** Polyacrylamide; emulsion polymerisation; Brij 35; hydrophilic polymer

*Received: October 2022; Accepted: December 2022*

Polyacrylamide (PAM) is a synthetic biodegradable polymer derived from acrylamide (AM) monomers. It is also known as a neurotoxin that was first used as an electrophoresis support matrix in 1959 (1,2). PAM is insoluble in most common organic liquids such as methanol, ethanol and acetone, but it is highly soluble in water. The solubility of PAM in aqueous solution is due to acid ( $-\text{COOH}$ ) and amide ( $-\text{CONH}-$ ) functionalities, which are extensively solvated by water. When PAM is crosslinked, it inflates in water instead of dissolving, and when hydrated, PAM absorbs a lot of water and forms a soft gel (3). PAM is hydrophilic, thus it has a strong affinity for water and may create very concentrated aqueous solutions. Despite its great hydrophilicity, PAM is mostly used in the flocculation of aqueous suspensions and as a flocculant in industrial and municipal water clarifying operations because of its gel-like characteristics (4). Furthermore, PAM and related hydrogels also have wide applicability in biomedical sciences, emphasizing the need for a better understanding of its biocompatibility characteristics and biological membrane functions (5).

There are various types of polymerisation techniques that can be implemented for the synthesis of hydrophilic polymers, such as bulk, solution,

suspension, and emulsion polymerisation, as well as irradiation polymerisation (6). Emulsion polymerisation is the simplest method which requires only the monomer, surfactant, monomer-soluble initiator and water as the dispersion medium. Furthermore, this allows for fast polymerisation to produce high molecular weight polymers with minimal polydispersity.

The surfactant plays a crucial function in emulsion polymerisation by reducing interfacial tension; this allows reactive vinyl monomers to emulsify and stabilise colloidal dispersions of nano-sized polymer particles (7). In emulsion polymerisation, the surfactant acts as an emulsifier and solubilises the monomer droplets. The surfactant must be able to produce a uniform dispersion and maintain its particle size and stability. The presence of a surfactant can reduce the surface tension between air and water or other immiscible liquids. This benefit can be achieved by rapidly converting water-insoluble polymers into emulsions (8).

Although hydrophobic monomers and the utilisation of anionic surfactants in emulsion polymerisation have good potential for medical and technology applications, further research is required to enhance the synthesis of hydrophilic monomers using

non-ionic surfactants via emulsion polymerisation (9). Non-ionic surfactants have been utilised in the emulsion polymerisation of polymer particles and provide several advantages over anionic surfactants, including improved chemical and freeze-thaw durability, increased pigment affinity, and reduced emulsion effervescence (10). Non-ionic surfactants have been observed to migrate from an aqueous medium into a monomer phase before emulsion polymerisation commenced. It has been reported that a non-ionic surfactant released from monomer droplets entered polymerising particles swollen with the monomer through the aqueous phase and persisted within these particles until polymerisation was complete (11).

Polyoxyethylene (23) dodecanol (Brij 35) is a non-ionic surfactant, where the sum of the lengths of the ethylene-oxide groups and the alkyl chain are equal to 35. Micelles are formed in water by non-ionic surfactants with a structure consisting of a hydrophilic part (polyethylene oxide chains) and a hydrophobic part (n-alkyl chains) (12). The contact between an uncharged polymer and an uncharged surfactant is typically thought to be weak; for instance, certain polymers have no interaction with polyethoxylated non-ionic surfactants (9). Brij 35 was selected for this study on account of its steric hindrance, equivalent availability, high purity, low cost, low toxicity, high cloud temperature and low background absorption. Furthermore, Brij 35 also showed remarkable stability during polymerization (13).

This study aimed to investigate the effects of different concentrations of Brij 35 surfactant on the emulsion polymerisation of PAM particles. The effects of different concentrations of the non-ionic surfactant on the formation of PAM particles are thoroughly discussed. The development of PAM particles using a non-ionic surfactant could bring new insights, especially for applications such as coatings, biomedicine, electrophoresis and drug delivery, where uncharged latexes (polymer emulsion) are required.

## EXPERIMENTAL

### Chemicals and Materials

Acrylamide (AM) monomer, Brij 35, and ammonium persulphate (APS) were all commercially purchased from Sigma Aldrich and used without further purification. Distilled water (DH<sub>2</sub>O) was used as the dispersion medium throughout the experiment.

### Synthesis of PAM via Emulsion Polymerisation

Emulsion polymerisation was conducted in a 250 mL three-neck round bottom flask that comprised a nitrogen gas inlet, a magnetic stirrer, a thermometer, and a reflux condenser. Initially, the AM monomer (0.28 g) and Brij 35 solution were combined with 6 mL double distilled water. The experiment was performed in the fume hood to protect from exposure

to potential chemical contamination. To remove any soluble oxygen, the solution was purged with N<sub>2</sub> for 15 minutes (14). The solution was then placed in a heating mantle and heated at 70 - 80 °C while stirring (100 rpm - 120 rpm). APS aqueous solution (0.91 mg) was added to the emulsion polymerisation after the reaction temperature reached 70 °C, and the reaction was kept at this temperature for 3 hours until polymerisation was completed. Then, the product was cooled to room temperature and excess water was removed by rotary evaporation. The synthesis was conducted three times using AM monomers prepared with different Brij 35 concentrations: below CMC, equivalent to CMC, and above CMC.

### Characterization Methods

#### Fourier Transform Infrared Analysis

All the IR spectra of PAM were recorded using the Invenio S Bruker FTIR spectrophotometer via Platinum Attenuated Total Resonance (ATR) with 16 scans in the spectral range of 6000-400 cm<sup>-1</sup>. From the IR spectra, the frequency and vibrational modes of the functional groups present in the compounds were determined.

#### Thermogravimetric Analysis

A Perkin-Elmer TGA Analyser (Q500 (TA Instrument)) was used for thermogravimetric analysis of the synthesised PAM as well as the AM monomers. TGA can also determine weight changes (gain or loss) in materials. The data revealed the material's thermal stability as well as its chemical analysis. A temperature range of 30 - 600 °C and a heating rate of 10 °C/minute under an argon atmosphere was used for the analysis.

#### Scanning Electron Microscopic Analysis

An Auto Fine Coater (JOEL) (SEM) was used to coat samples with fine-grained gold for scanning electron microscopy (SEM) imaging using JSM-6360 LA to record the surface morphological changes of the PAM samples. The SEM used 10 kV accelerated voltage and provided magnification from 250x to 3500x.

## RESULTS AND DISCUSSION

### Synthesis of PAM via Emulsion Polymerisation

PAM was successfully synthesised via emulsion polymerisation using polyoxyethylene (23) dodecanol (Brij 35) as a non-ionic surfactant at various concentrations. The effects of surfactant concentration on particle size and the formation of polymer particles were investigated, and the samples involved in this study are listed in Table 1. It is worth noting that the concentrations of Brij 35 were selected based on previous studies (15-18). Three different concentrations of Brij 35 were selected at below critical micelle concentration (CMC), equivalent to CMC, and above

CMC to observe its effects on the formation and stability of PAM.

At first, all the reactants produced colourless solutions that were water soluble. The polymerisation process required high quality monomers and initiators in the absence of oxygen. The interaction between monomer and surfactant can produce micelles if the amount of surfactant added is above the CMC. A micelle may become the locus of polymerization due to its larger size, as it is more likely to capture aqueous phase radicals generated by an initiator (19).

The addition of Brij 35 was observed to change the rate of PAM polymerization. The polymerisation rate slowed when the concentration of Brij 35 increased in the pre-gel solution. The viscosity of all three samples varied depending on the concentration

of Brij 35 added. After polymerisation, the PAM particles were in the form of a liquid gel, which was then dried at room temperature for 24 hours to form the final product, which was a solid wet hydrogel (Figure 1).

#### Fourier Transform Infrared Analysis

To validate the formation of PAM, FTIR analysis was performed to determine the functional groups of the synthesized polymers PAM\_1, PAM\_2 and PAM\_3, compared to its acrylamide (AM) monomer. Figure 2 shows the IR spectrum of the AM monomer while Figure 3 depicts the FTIR spectra of PAM prepared using Brij 35 at different concentrations. The IR spectrum of the AM monomer (Figure 2) exhibited the absorption bands of the  $\nu(\text{C-H})$ ,  $\nu(\text{C=O})$ , and  $\nu(\text{CH}_2)$  functional groups.

**Table 1.** PAM Nanoparticles Prepared at Different Concentrations of Brij 35.

Polymer Sample	Concentration of Brij 35 (mM)
PAM_1	0.06 (below CMC)
PAM_2	0.09 (equivalent CMC)
PAM_3	0.12 (above CMC)



**Figure 1.** Physical Appearance of (a) PAM\_1, (b) PAM\_2, and (c) PAM\_3

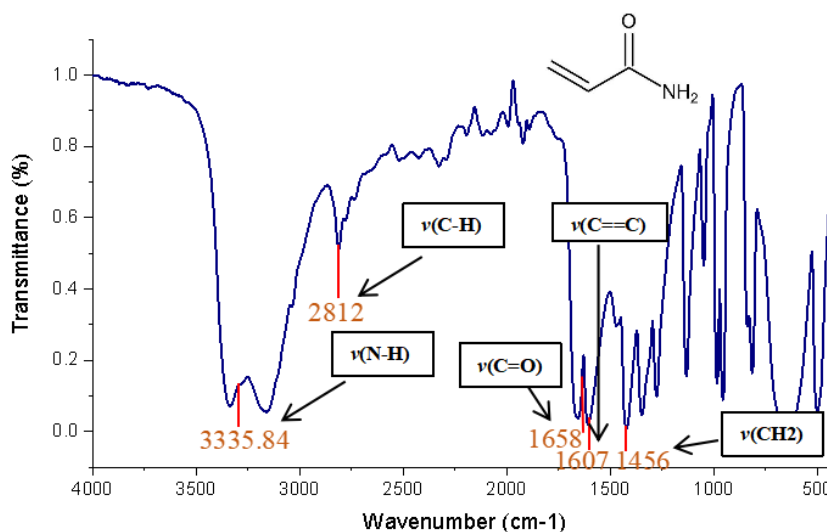


**Figure 2.** IR spectrum of the acrylamide (AM) monomer

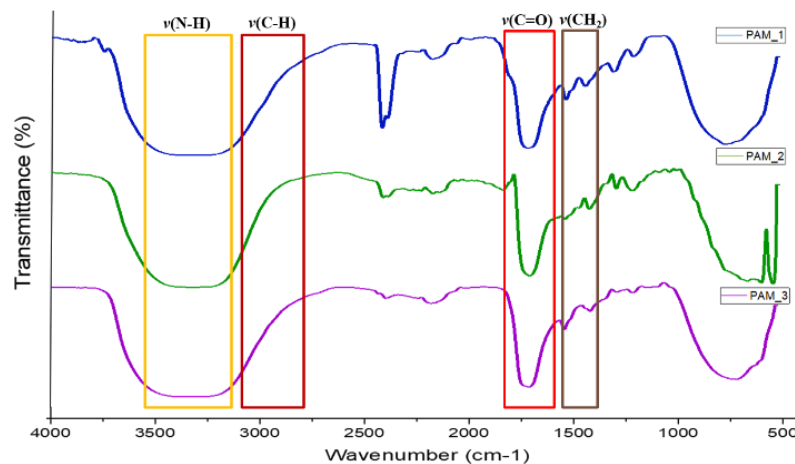


**Figure 3.** IR Spectra for PAM\_1, PAM\_2, and PAM\_3

Broader peaks were observed in the spectra of all the PAM samples (Figure 3). The secondary amide  $\nu(\text{C}=\text{O})$  stretching absorption band appeared at  $1638\text{ cm}^{-1}$  (20). The CH stretching of the  $\nu(\text{C}-\text{H})$  and  $\nu(\text{CH}_2)$  absorption peaks were presented at  $2924\text{ cm}^{-1}$  and  $1465\text{ cm}^{-1}$ , respectively. These IR peaks were in agreement with previous studies (21, 22). Most importantly, the presence of a broad peak at  $3326\text{ cm}^{-1}$  was due to  $\nu(\text{N}-\text{H})$  stretching. The peak at  $3348 - 3202\text{ cm}^{-1}$  which showed a strong or medium intensity of symmetrical ( $\nu_{\text{sym}}$ ) and antisymmetrical ( $\nu_{\text{asym}}$ ) N-H stretch was produced by the presence of intermolecular hydrogen bonding, which can be seen as broadening and spectral complexity in the unresolved bonds (22). Intra- and inter-chain hydrogen bonds of  $\text{N}-\text{H}\dots\text{O}=\text{C}$  were formed by the  $\text{NH}_2$  groups (23). In addition, the disappearance of the  $\nu(\text{C}=\text{C})$  bond which typically appeared around  $1607\text{ cm}^{-1}$  demonstrated that the acrylamide monomer had been entirely transformed to polyacrylamide, with no monomers remaining (24). Furthermore, all the functional groups of interest in the polyacrylamide (PAM) samples showed frequency shifts relative to the monomer.

### Thermogravimetric Analysis

TGA is a popular approach for the determination of kinetic parameters such as activation energy, pre-exponential factor and reaction order, as well as for investigating the thermal degradation of polymers (24). In this study, TGA was used to determine the thermal stability of PAM by measuring polymer weight loss as a function of temperature. The AM monomer and PAM\_2 nanoparticles were analysed under argon gas with a flow rate of  $60\text{ mL/min}$  and a heating rate of  $10\text{ }^\circ\text{C/min}$ , from  $30 - 600\text{ }^\circ\text{C}$ . PAM\_2 nanoparticles which used  $0.09\text{ mM}$  of Brij 35 were chosen for the analysis due to their stability during the polymerisation process in comparison to PAM\_1 and PAM\_3.

From the thermogram in Figure 4, the AM monomer showed three stages of thermal degradation, where the onset temperature was  $40\text{ }^\circ\text{C}$ . When the temperature approached  $216.67\text{ }^\circ\text{C}$ , a second degradation was recorded, which might be due to traces of moisture within the samples. The third degradation

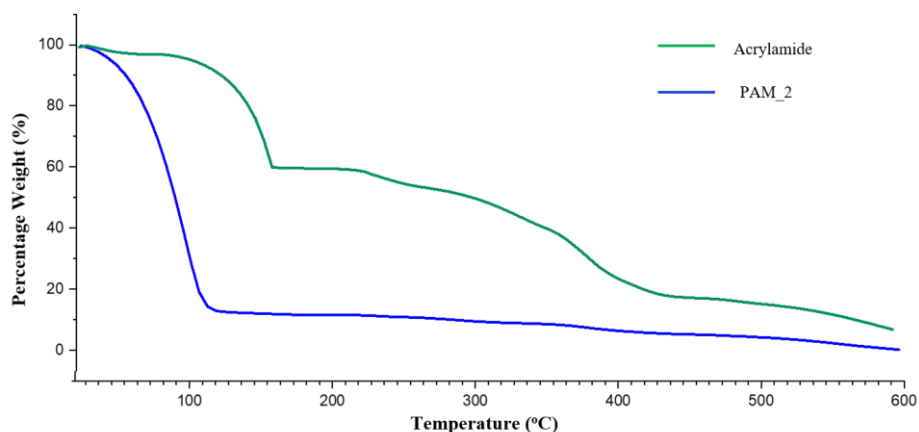


**Figure 4.** Thermograms of the AM monomer and PAM\_2.

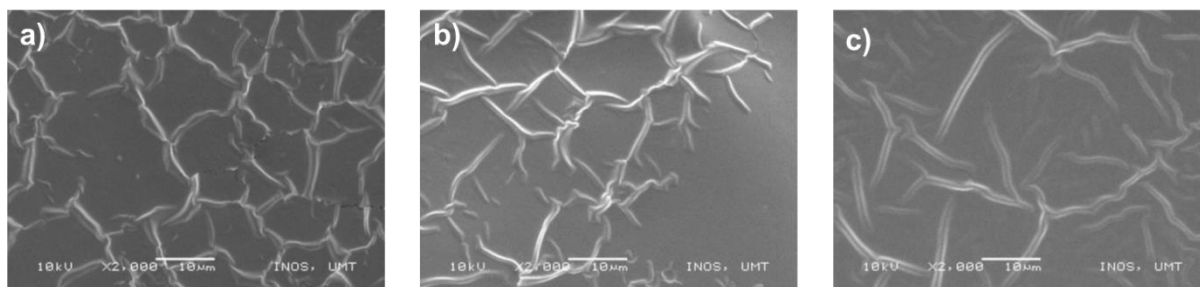


**Figure 5.** SEM Images of (a) PAM\_1 (b) PAM\_2, and (c) PAM\_3 at 2000x magnification

stage was observed at 432.50 °C. The AM monomer completely degraded when the temperature reached 500 - 600 °C. On the other hand, PAM\_2 showed two stages of thermal degradation. The first stage was observed at 30 °C, while the second stage occurred when the temperature reached 333.33 °C. These two stages in the PAM\_2 thermogram may be due to the release of ammonia from the imidisation reaction between the monomer unit's amide groups, followed by the breakdown of the polymer backbone and the imides generated in the first decomposition (25). From the thermogram in Figure 4, there was no indication of water in the sample. PAM\_2 started to degrade completely after the temperature reached 595.83 °C. PAM\_2 and the AM monomer showed weight losses of 5.15 % and 7.78 %, respectively. The results indicate that PAM\_2 required a lower temperature for weight loss compared to the monomer.

### Scanning Electron Microscopy Analysis

A tabletop SEM was utilised to observe the surface morphology of the synthesised PAM particles. Pristine PAM hydrogels are thought to have a morphology comprising of relatively bulb-like structures connected by slender fibrils (26). However, from the SEM micrographs, the images of the PAM particles, as shown in Figure 5, revealed a morphology that was different to that previously described.

PAM\_1 showed a structure that consisted of multitudinous spherical units in random aggregation, while PAM\_2 revealed the existence of a micro-structure as well as fibril-like structures forming on the surface of the PAM hydrogels. The morphology of PAM\_3 on the other hand revealed a parallel leaflet structure. As a result, it is likely that different concentrations of Brij 35 used in the polymerization affect the shape of the PAM particles produced. The average particle size of PAM was estimated by randomly measuring the polymer particles acquired from SEM images, and the average particle size of PAM particles was determined to be in the range of 5 - 100 μm with substantial aggregations. Due to the nature of the sample preparation for SEM and the drying process of the samples, the aggregation of polymer materials was expected to be observed.

### CONCLUSION

Emulsion polymerization of polyacrylamide (PAM) with concentrations of Brij 35 at below, equivalent, and above CMC, was successfully achieved. The formation of PAM was confirmed by FTIR analysis, in which significant peaks due to  $\nu(\text{N-H})$  were observed at 3326  $\text{cm}^{-1}$ . Despite being unable to clearly observe the morphology and structure of the polymer due to the limitations of SEM, the existence of fibril-like structures were observed in the PAM samples. Thermograms obtained from the TGA analysis illustrated multistage mass changes throughout the temperature range of 0 - 600 °C in which PAM\_2 exhibited the highest temperature at which mass changes occurred. Therefore, it can be concluded that the concentration of Brij 35 nonionic surfactant used in polymerization affected the morphology and thermal properties of the PAM produced.

### ACKNOWLEDGEMENTS

We thank the Ministry of Higher Education, Malaysia for the funding (FRGS/1/2020/STG02/UMT/02/1 – FRGS Vot Code 59633) and Universiti Malaysia Terengganu for their generous support.

### REFERENCES

1. Bera, A. & Belhaj, H. (2016) Application of Nanotechnology by Means of Nanoparticles and Nanodispersions in Oil Recovery – A Comprehensive Review. *Journal of Natural Gas Science and Engineering*, **34**, 1284–1309.
2. Bashir, S., Hina, M., Iqbal, J., Rajpar, A. H., Mujtaba, M. A., Alghamdi, N. A., Wagesh, S., Ramesh, K., and Ramesh, S. (2020) Fundamental Concepts of Hydrogels: Synthesis, Properties and Their Applications. *Polymers*, **12**, 2702.
3. Herth, G., Schornick, G. & Buchholz, F. L. (2015) Poly(Acrylamides) and Poly(Acrylic Acids). *Ullmann's Encyclopedia of Industrial Chemistry*, **28**, 1–16.
4. Zielińska, A., Carreiró, F., Oliveira, A. M., Neves,

- A., Pires, B., Venkatesh, D. N., Durazzo, A., Lucarini, M., Eder, P., Silva, A. M., Santini, A. & Souto, E. B. (2020) Polymeric Nanoparticles: Production, Characterization, Toxicology and Ecotoxicology. *Principles of Nanomedicine*, **25(16)**, 195–240.
5. Ormategui, N., Zhang, S., Loinaz, I., Brydson, R., Nelson, A. & Vakurov, A. (2012) Bioelectrochemistry Interaction of Poly(N-isopropylacrylamide) (pNIPAM) Based Nanoparticles and Their Linear Polymer Precursor with Phospholipid Membrane Models. *Bioelectrochemistry*, **87**, 211–219.
  6. Ahmed, E. M. (2015) Hydrogel: Preparation, Characterization, and Applications: A Review. *Journal of Advanced Research*, **6(2)**, 105–121.
  7. Ahmed, E. M. (2015) Hydrogel: Preparation, Characterization, and Applications: A review. *Journal of Advanced Research*, **6(2)**, 105–121.
  8. Azmi, N. S., Kamaruddin, N. N., Kassim, S. & Harun, N. A. (2018) Synthesis and Characterization of Hydrophilic Polymer Nanoparticles Using n-isopropylacrylamide (NIPAM) via Emulsion Polymerization Technique. *IOP Conference Series: Materials Science and Engineering*, **440(1)**, 1–6.
  9. Tóth, G. & Madarász, A. (2006) Structure of Brij-35 Nonionic Surfactant in Water: A Reverse Monte Carlo Study. *Langmuir*, **22(2)**, 590–597.
  10. Wijting, W. K., Laven, J., Van Benthem, R. A. T. M. & De With, G. (2008) Adsorption of Ethoxylated Styrene Oxide and Polyacrylic Acid and Mixtures Thereof on Organic Pigment. *Journal of Colloid and Interface Science*, **327(1)**, 1–8.
  11. Matsusaka, N., Suzuki, T. & Okubo, M. (2013) Effect of Partitioning of Monomer and Emulsifier in Aqueous Media on Particle Formation in Emulsion Homopolymerization of Hydrophobic and Hydrophilic Monomers with a Nonionic Emulsifier. *Polymer Journal*, **45(2)**, 153–159.
  12. Fernandez, A. M. & Jebbanema, L. (2007) The effect of Surfactant Selection on Emulsion Polymer Properties. *Paint & Coatings Industry*. <https://www.pcimac.com/articles/87271-the-effect-of-surfactant-selection-on-emulsion-polymer-properties>
  13. Borgerding, M. F. & Hinze, W. L. (1985) Characterization and Evaluation of the Use of Nonionic Polyoxyethylene (23) Dodecanol Micellar Mobile Phases in Reversed-Phase High-Performance Liquid Chromatography. *Analytical Chemistry*, **57(12)**, 2183–2190.
  14. Shalviri, A., Chan, H. K., Raval, G., Abdekhodaie, M. J., Liu, Q., Heerklotz, H. & Wu, X., Y. (2013) Design of pH-Responsive Nanoparticles of Terpolymer of Poly(methacrylic acid), Polysorbate 80 and Starch for Delivery of Doxorubicin. *Colloids and Surfaces. B: Biointerfaces*, **101**, 405–413.
  15. Alina, S. K., Eric, R., Yuri, A. A., Alexey, A. L., Anastasiya, O. K., Natalia, A. S., Evgenia, A. S. & Irina, S. (2018) Mixed Aqueous Solutions of Nonionic Surfactants Brij 35/Triton X-100: Micellar Properties, Solutes' Partitioning from Micellar Liquid Chromatography and Modelling with COSMOmic. *Colloids and Surfaces A: Physicochemical and Engineering Aspects*, **538**, 45–55.
  16. Zahari, V., Katev, V., Radeva, D., Tcholakova, S. & Denkov, N. D. (2018) Micellar Solubilization of Poorly Water-Soluble Drugs: Effect of Surfactant and Solubilizate Molecular Structure. *Drug Development and Industrial Pharmacy*, **44(4)**, 677–686.
  17. Hait, S. K. & Moulik, S. P. (2001) Determination of Critical Micelle Concentration (CMC) of Nonionic Surfactants by Donor-Acceptor Interaction with Iodine and Correlation of CMC with Hydrophile-Lipophile Balance and Other Parameters of the Surfactants. *Journal of Surfactants and Detergents*, **4**, 303–309.
  18. Ali, A., Malik, N. A., Farooq, U., Tasneem, S. and Nabi, F. (2016) Interaction of Cetrимide with Nonionic Surfactants—Triton X-100 and Brij-35: A Conductometric and Tensiometric Study. *Journal of Surfactants and Detergents*, **19 (3)**, 527–542.
  19. Zhang, S., Shi, Z., Xu, H., Ma, X., Yin, J. & Tian, M. (2016). Revisiting the Mechanism of Redox Polymerization to Build the Hydrogel with Excellent Properties using a Novel Initiator. *Soft Matter*, **12(9)**, 2575–2582.
  20. Muhamad, I. I., Asgharzadehahmadi, S. A., Zaidel, D. N. A. & Supriyanto, E. (2013) Synthesis and Characterization of Polyacrylamide Based Hydrogel Containing Magnesium Oxide Nanoparticles for Antibacterial Applications. *International Journal of Biology and Biomedical Engineering*, **7(3)**, 108–113.
  21. Singh, R., Kant, K. & Mahto, V. (2015) Study of the Gelation and Rheological Behavior of Carboxymethyl Cellulose-Polyacrylamide Graft Copolymer Hydrogel. *Journal of Dispersion Science and Technology*, **36(6)**, 877–884.
  22. Dweik, H., Sultan, W., Sowwan, M. & Makharza,

- S. (2008) Analysis Characterization and Some Properties Of Polyacrylamide Copper Complexes. *International Journal of Polymeric Materials and Polymeric Biomaterials*, **57(3)**, 228–244.
23. Mya, K. Y., Jamieson, A. M. and Sirivat, A. (1999) Interactions Between the Nonionic Surfactant and Polyacrylamide Studied by Light Scattering and Viscometry. *Polymer*, **40(21)**, 5741–5749.
24. Shatat, R. S., Niazi, S. K. and Ariffin, A. (2017) Synthesis and Characterization of Different Molecular Weights Polyacrylamide. *IOSR Journal of Applied Chemistry*, **10(04)**, 67–73.
25. Yang, M. H. (1998) Two-Stages Thermal Degradation of Polyacrylamide. *Polymer Testing*, **17(3)**, 191–198.
26. Ruchel, R. & Brager, D. M. (1975) Scanning Electron Microscopic Observations of Polyacrylamide Gels. *Analytical Biochemistry*, **68**, 415–428.